Performance Evaluation of DualSPHysics and COMCOT Programs through Numerical Testing for Simulating Tsunami Propagation and Overtopping on Seawalls

Ahmad Bagus Reza Zuliansah[1*], *Umboro Windujati*[1], *Teuku Muhammad Rasyif*[2], *Teuku Mahlil*[1], *Nurul Fajar Januriyadi*[1]

[1]Civil Engineering, Faculty of Infrastructure Planning, Pertamina University, Teuku Nyak Arief Street, South Jakarta, DKI Jakarta, 12220, Indonesia

[2]Civil Engineering, Faculty of Engineering and Computer Science, Bakrie University, Rasuna Epicentrum District, HR Rasuna Said Street, Kuningan, DKI Jakarta, 12940

Abstract. A tsunami is a destructive wave that can cause massive damage to coastal infrastructure. One of the disaster mitigation measures that can be chosen is the construction of coastal protection infrastructure, such as a seawall. Seawalls play a crucial role in protecting coastal areas as they can reduce wave energy and minimize the impact of tsunami-induced damage. However, during the 2011 Japan tsunami, the seawall built in Taro city failed as it proved to be less effective in handling the tsunami waves. The research conducted aims to model the propagation and overtopping of tsunami waves on the seawall, initially carried out through physical laboratory experiments, and later transformed into numerical test models using the Smoothed Particle Hydrodynamics (SPH) method and the Cornell Multigrid Coupled Tsunami (COMCOT) model. In this study, the parameters being compared include wave height, wave propagation, and overtopping on the seawall under two scenarios : the run-up of solitary waves on a shore without a seawall and the overtopping condition with a seawall using the Solitary Wave generation type, following the experiments conducted by Huang et al en 2022. Several parameters in the laboratory case study should be considered to expand our understanding of the systematically discussed tsunami propagation and overtopping processes and evaluate the capabilities of the SPH and COMCOT models.

Keywords: *Tsunami, Seawall, Propagation, Overtopping, DualSPHysics, COMCOT*

1 Introduction

1.1 background

Tsunamis are destructive waves caused by earthquakes, volcanic eruptions, underwater landslides, or due to meteor impacts [1]. Despite their initial height of tsunami is only one meter in deep sea conditions, these waves exhibit high propagation speeds as they approach coastal areas, resulting in a significant reduction in wavelength and a corresponding increase in wave height [2]. In coastal regions, tsunami waves can reach heights of ten meters, causing extensive damage. Consequently, tsunamis represent a risk that threatens the life and safety communities residing in coastal areas. The Japanese tsunami in 2011 which inflicted extensive devastation along the coastline, extending as far as 11.3 km inland, resulted in a tragic toll of 14,508 fatalities, 11,452 individuals reported as missing, more than 162,000 buildings damaged, and 300 bridges severely affected [3][4].

The 2011 Japanese tsunami was effectively mitigated due to the presence of tsunami gates, with a height of 15.5 meters, at the mouth of the Fudai river [5]. These tsunami gates successfully shielded the Fudai area from a 17-meter tsunami and overtopping that extended several meters, all while withstanding minimal damage, thereby preventing inundation, and safeguarding the populated regions. Without these tsunami gates, the tsunami could have inundated and wreakde havoc in Fudai area because the topological features, surrounded by cliffs, would have allowed the accumulation and concentration of tsunami energy, resulting in more significant devastation [5]. However, in other areas like Taro, the protection provide by seawalls was not as effective, leading to a significant loss of life and seawall overtopping. Several factors contributed to the failure of seawall structures, including their X-shaped design, which concentrated tsunami energy at the center wall, the fact that they were not

*Corresponding authors : bagusreza2113@gmail.com

designed to withstand a magnitude Mw = 9 earthquake, issues with maintenance and inter-wall connection, and a lack of community awareness due to false sense of security provided by the seawall [5]. Consequently, studying the performance of coastal protection structures, particulary seawalls, and implementing non-structural mitigation measures such as education, urban planning, and insurance, becomes crucial [5].

Based on previous research, numerous studies have been conducted on the effectiveness of seawalls against tsunamis and generation of tsunamis, specifically solitary waves or dam-breaks [6]. These investigations can be carried out using various methods, including laboratory tests, numerical simulations, and analytical approaches. However, there are several limitations associated with laboratory testing, such as significant cost, time constraints, and the need for substantial manpower, especially when alterations to the flume, which can restrict the scope and efficiency of the research [7]. Research conducted using numerical methods can provide more complex geometric modeling compared to laboratory tests. Numerical methods are capable of solving systems of non-linear equations and handling complex geometries that practically impossible to address analytically or in a laboratory setting [8]. In the modeling of tsunami, two common generation methods are frequently utilized in research : solitary wave or solitons, and dam-break events. The first method involves the generation of waves resulting from the sudden breach or dam-break of dam. Dam-break flow are not employed to assess dam failures, but can also be used to study tsunamis as demonstrated by Li, Y [9] [10]. This is due to the similarity between tsunami propagation toward the coast and waves generated by dam-break events. The mechanism involves the releases of water volume from a reservoir above a low-lying surface [11]. The second methode involves the generation of solitary wave. Solitary waves are a wave phenomenon that occurs when a tsunami which can maintain its shape with high speed velocity and high amplitude. Tsunami simulation using solitary wave generation often employ wave drivers or wave makers [12].

The *DualSPhysics*are program is a numerical model in 2 and 3 dimensions that apply *Smoothed Particle Hydrodynamics* (SPH) to simulate fluids using small particles. In its application, *SPH* is used to simulate wave propagation, wave breaking, the influence of waves on dam-break events, and various structures, including seawall [13]. *SPH* offers advantages over other models such as mesh-based model, due to its gridless nature, resulting in faster computation times compared to mesh-based method [14]. Given its advantages, *SPH* modeling has been widely adopted by researchers worldwide in coastal engineering for wave related problems, delivering excellent results with high levels of accuracy and validation against experimental data [14]. However, it is worth nothing that computational times for *SPH* simulating are longer when compared to simulations conducted using Comcot.

COMCOT modeling can be employed for the simulation of *near-field* tsunamis generated by seafloor deformation and submarine avalanches utilizing the principles of linear dislocation theory. The COMCOT model incorporates the Shallow Water Equation, which utilizes a *leapfrog* scheme coupled with a *multi-grid* system, featuring up to 12 *sub-level* grids. [15]. The foundation of the COMCOT equation rest upon the mass and momentum conservation equations, encompassing both *linear* and *nonlinear* shallow water equations. These equations find widespread use in numerical studies, facilitating the analysis of how wave height and velocity change in response to alterations in ocean geometry. The *Shallow Water Equations* (SWE) can be effectively solved numerically, with the *Finite Element Method* being the most utilized technique in numerical test. However, for the purposes of this study, a simpler approach, the *Finite Difference Method,* will be employed. Numerous studies leveraging COMCOT numerical simulations have significantly contributed to the field of tsunami modeling. For instance, one research study focused on reconstructing the Mentawai tsunami event, aiming to validate tsunami *run-up* height by comparing the findings of field studies conducted by the GITST Team in 2010 [16]. Additionally, another numerical investigation, pertaining to the 2004 *Indian Ocean Tsunami* conducted by [17], centered on researching land separation due to hydrodynamic forces and the resulting *overtopping* phenomenon in the Ujong Seudeun area, induced by the tsunami.

Numerical testing plays a pivotal role in the development and initial design phases of seawalls designed to provide protection against natural disasters, particularly flooding, coastal erosion, and tsunami inundation. Consequently, the *seawall* numerical testing undertaken in this study directed at assessing the capability of the *DualSPHysics* (SPH) and *Cornell Multigrid Coupled Tsunami* (COMCOT) programs in modeling *overtopping* and wave propagation on seawalls induced by tsunami events. The outcomes derived from the *DualSPHysics* (SPH) and COMCOT modeling assessments are intended to validate the effectiveness of these programs in conducting simulations, aiming for superior results. The significance of validation lies in its potential application for laboratory-based studies and evaluations of seawall performance. Furthermore, it serves as a valuable resource for future researchers, assisting them in modeling wave interactions with seawall structures to design robust structures capable of withstanding lift and hydrodynamic loads. Moreover, this research can serve as a reference point for other researchers engaging in tsunami simulations through numerical testing methodologies. Beyond its academic value, this study is expected to represent the initial steps toward practical tsunami disaster mitigation by examining the effectiveness of a *seawall* design in safeguarding against tsunami events in real-world scenarios.

2 method

2.1 *Smoothed Particle Hydrodynamics* (SPH)

*DualSPhysics*is is a numerical model that employs the Smoothed Particle Hydrodynamics (SPH) method. In this model, fluids, boundaries, and solids objects are represented as particles, and the interactions between neighboring particles depend on the distance between them. To compute this interaction, the kernel function (W) is utilized, which is influenced by the smoothing length (h). The function $f(r)$ is defines the influences of one particle on another, with distance being a crucial sensitivity factor in this context. When the distance is small, the influence on one another becomes more significant, and conversely, as the distance increases, the influence diminishes. The following is an equation that describes the function $f(r)$:

$$f(r) = \int f(r')W(r - r', h)dr \quad (1)$$

where, $f(r)$ represents the mean value, W denotes the kernel function, and h is the smoothing radius. The value of h govern theextent of the región surrounding a particle that will affect the physics calculations on that particle. When this function is interpolated within a particle, Equation 2 is obtained:

$$f(r_a) \approx \sum_b f(r_b)W(r_a - r_b, h)\Delta v_b \quad (2)$$

Where, r the subscripts a and b represent individual particles, Δv respresent the volume of particles b. As volume is the density ratio, Equation 3 becomes :

$$f(r_a) \approx \sum_b f(r_b)W(r_a - r_b, h)\left(\frac{m_b}{\rho_b}\right) \quad (3)$$

where, m_b and ρ_b respresent the mass and density of particle b respectively. The accuracy of SPH analysis relies on the choice of the kernel function. The function is defined as $q = \frac{r}{h}$. Here, r is the distance between the two particles and q is the dimensionless ratio. The definition of the Wendland kernel function used in this study is as follows:

$$W(r, h) = a_D\left(1 - \frac{q}{2}\right)^4 (2q + 1) \quad (4)$$

where the value a_D is 7/4 πh2 for 2D analysis and 21/16 πh3 for 3D analysis.

The mass conservation equation, or continuity, is employed to quantify density variations:

$$\frac{d\rho_a}{dt} = \sum_b m_b\, v_{ab}.\nabla_a W_{ab} \quad (5)$$

The relationship between pressure and density is provided by the following equation:

$$p = b\left(\frac{\rho}{\rho_0}\right)^\gamma - 1 \quad (6)$$

$$b = c_0^2\rho_0/\gamma \quad (7)$$

where, $\gamma = 7$ and $\rho_0 = 1000$kg/m3. c_0 represents the speed of sound.

The speed of sound (c_0) is numerically calculated using at least ten times the maximum velocity within the system. For dam-break flows, the equation for calculating the initial wave speed is as follows:

$$c_0 = c_s\sqrt{gh_w} \quad (8)$$

where, c_s represents the sound coefficient. h_w represents the fluid depth.

2.2 Cornel Multigrid Coupled Tsunami (COMCOT)

The research methodology employed in this study center on the utilization of the Cornell Multigrid Coupled Tsunami (COMCOT) software for the simulation tsunami waves. This approach involves the application of a 2-Dimensional Horizontal (2DH) modeling technique. The COMCOT program has demonstrated its capacity to conduct simulations with high accuracy and efficiency, as evidenced in the case of the Indian Ocean tsunami [18]. This software has the capability to numerically replicate the behavior of tsunami waves, offering a visual representation of how these waves propagate from the initial earthquake epicenter to the adjacent coastal areas. To achieve this, the approach employs the Shallow Water Equations (SWE), which encompass equations related to momentum and mass conservation. These equations are then discretized using the leapfrog and upwind methods. This discretization takes place in both spatial and temporal dimensions, accommodating both linear and nonlinear variations in spherical and Cartesian coordinates. The SWE equations can be written as follows [15].

$$\frac{\partial d}{\partial t} + \left\{\frac{\partial P}{\partial x} + \frac{\partial Q}{\partial y}\right\} = -\frac{\partial d}{\partial t} \quad (9)$$

$$\frac{\partial P}{\partial t} + \frac{\partial}{\partial x}\left\{\frac{P^2}{H}\right\} + \frac{\partial}{\partial y}\left\{\frac{PQ}{H}\right\} + gH\,\frac{\partial \eta}{\partial x} + F_x = 0 \quad (10)$$

$$\frac{\partial Q}{\partial t} + \frac{\partial}{\partial x}\left\{\frac{PQ}{H}\right\} + \frac{\partial}{\partial y}\left\{\frac{Q^2}{H}\right\} + gH\,\frac{\partial \eta}{\partial Y} + F_Y = 0 \quad (11)$$

While η represents the elevation of the water surface (m), t signifies the passage of time (s). In the same vein, d denotes the water depth (m), while P and Q symbolize the fluxes in the horizontal (x) and vertical (y) directions (m3/s). The coefficient f corresponds to the Coriolis force, H stands for the overall water depth (m), and Fx and Fy refer to the forces exerted by bottom friction in the horizontal (x) and vertical (y) directions.

2.3 Secondary Data

In this study, to demonstrate the capability of the DualSPHysics model in simulating tsunami propagation and seawall overtopping, the required data includes secondary data obtained from laboratory research conducted by Huang et al [19]. Table 1 outlines the research scenarios for conducting simulations.

Table 1. Summary of Simulation Scenario

Tipe Flume	Setup	Depth	Wave Height/Depth (H/h) (m)	H (m)	Scenario
without a seawall	1	1.2	0.338	0.4056	1
	2	2.2	0.152	0.3344	2
with a seawall	3	0.5	-	0.1	3

a. Flume size and Initial conditions

- Solitary wave run-up process on seawall-free beach (Setup 1 and Setup 2)

In Figure 1, the first computational setup for solitary wave run-up on a plain beach is based on measurements conducted by Hsiao et al. [20]. In Setup 1, a comparison of time with different water surface elevations for the generated waves, i.e., H/h = 0.338, will be obtained. Meanwhile, in Setup 2, H/h is set to 0.152. The shoreline is located 50 meters from the wave generator, and the beach slope is 1:60, as depicted in Figure 1. Twelve wave gauges (WG) are arranged along the wave flume at positions x = 50.0, 56.48, 62.96, 69.44, 75.92, 82.4, 89.6, 96.08, 102.56, 109.04, 115.52, and 122.0 meters for Setup 1. In Setup 2, sixteen wave gauge (WG) positions are used, namely at x = 24.0, 36.0, 50.0, 64.0, 78.0, 92.0, 106.0, 120.0, 130.0, 140.0, 148.0, 156.0, 164.0, 172.0, 182.0, and 194.0 meters. The computational domain has a length of 300 meters. In the simulations, the initial conditions for Setup 1 include a water depth (h) of 1.2 meters. For Setup 2, the initial condition is a water depth of 2.2 meters.

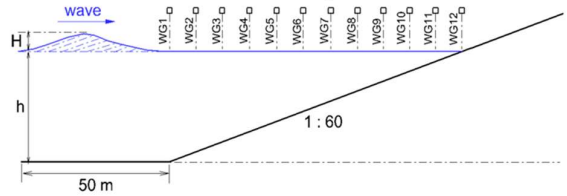

Fig. 1. Layout for Solitary Wave Runup Computation on a Plane Beach by Huang et al [19]

- *Solitary Wave Overtopping* on Seawall (Setup 3)

Figure 2 depicts the setup used to test the performance of the seawall against tsunami waves, in accordance with experimental data conducted by Hunt [21] at the UK Coastal Research Facility. The seawall is situated on a shoreline with a 1:20 slope, and the shoreline is located 8.33 meters from the wave paddle. The seawall itself is positioned 8.125 meters from the shoreline, with a seawall slope of 1:2. The computational domain has a length of 20 meters. The tranquil water depth (h) is set at 0.5 meters, while the wave event's height (H) is 0.1 meters. Wave gauges (WG) are installed at x = 8.33, 10.33, 12.33, 14.83, and 16.92 meters. This setup is employed to examine the propagation, transformation, run-up, and overtopping processes of solitary waves over the seawall. The flume used in the study conducted by Huang et al. [19] is provided below:

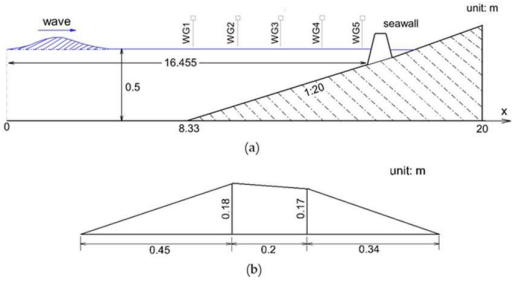

Fig. 2. Experimental Layouts; (a) Overall Layout; (b) Seawall Geometry Dimension by Huang et al [19]

b. Digitize water surface elevation data and overtopping.

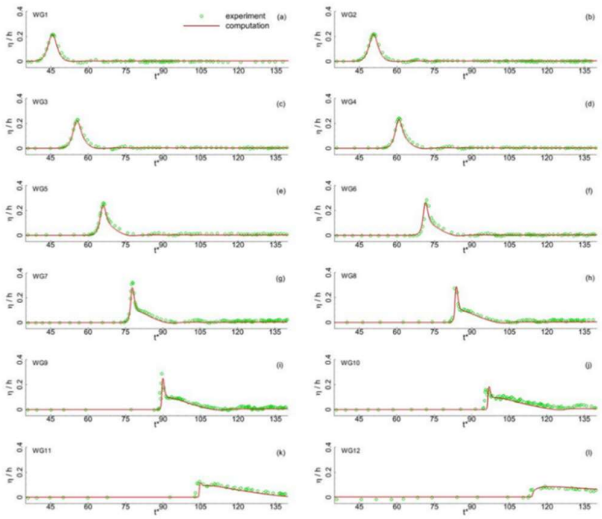

Fig. 3. Presents a Time Series Comparison with Water Surface Elevation at Different Wave Gauges (WG) for H/h = 0.338 at 12 WG by Huang et al [19] for Setup 1

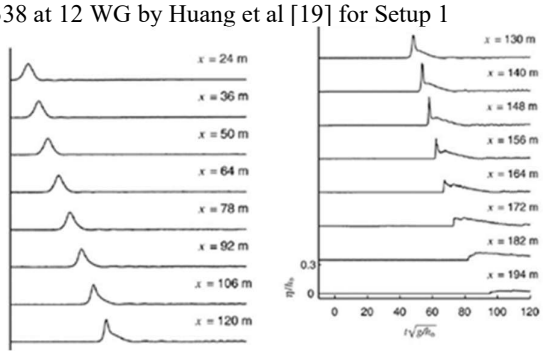

Fig. 4. Provide a Time Series Comparison with Water Surface Elevation at 16 Different Surge Gauges (WG) for H/h = 0.152 (Setup 2)

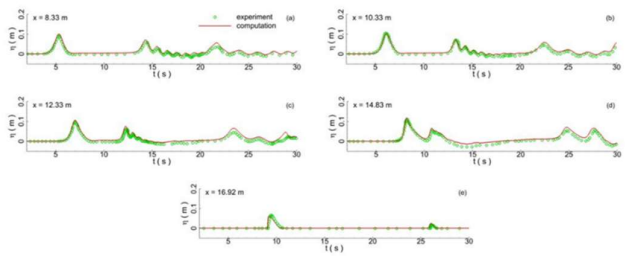

Fig. 5. Time Series Comparison of Overtopping on the Seawall; (a) t = 9 seconds; (b) t = 10 seconds; (c) t = 11 seconds; (d) t = 12 seconds; (e) t = 13 s. Huang et al [19] on setup 3

Secondary data for water surface elevation and overtopping were subjected to digitization processes to validate observational data against simulation results. This digitization process was carried out with the assistance of ArcGIS.

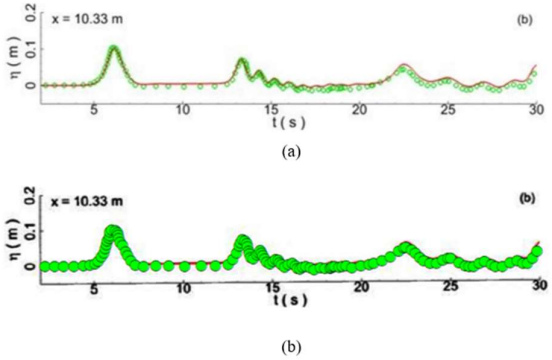

Fig. 6. Graph of Time Series Comparison with Water Surface Elevation at Wave Gauge WG2 (a) Before Digitization and (b) After Digitization.

2.4 Setup Model

In this Setup model, data input was performed using a programming language to enable the simulation to run. In DualSPHysiscs, data input process involved using software Notepad++ to modify the DualSPHysisc program to suit the specific research case. The required data includes simulation area, constants, parameters, initial conditions, wave generation, and observation points. Subsequently, the results were obtained from DualSPHysics for each setup, presented in 2D as shown in Figure 7 through Figure 9.

2.5 Validation Testing of Simulation Model against Experimental Results

In testing this model, 4 different validation methods were employed: Root Mean Square Error (RMSE), and Mean Absolute Error (MAE), Nash-Sutcliffe efficiency (NSE), and RMSE-observations standard deviation ratio (RSR). Small and close-to-zero values of RMSE and MAE indicated improved predictions or simulations that closely resemble the real conitions. Meanwhile, NSE and RSR have categories as outlined in table 2.1, seving as reference for prediction or simulation results falling into specific categories.

$$RMSE = \sqrt{\frac{1}{N}\sum_{i=1}^{N}(Y_i - Y_i')^2} \tag{9}$$

$$MAE = \frac{1}{N}\sum_{i=1}^{N}|Y_i - Y_i'| \tag{10}$$

$$NSE = 1 - \frac{\sum_{i=1}^{n}(Y_i^{obs} - Y_i^{sim})^2}{\sum_{i=1}^{n}(Y_i^{obs} - Y^{mean})^2} \tag{11}$$

$$RSR = \frac{RMSE}{STDEV_{obs}} = \frac{\sqrt{\sum_{i=1}^{n}(Y_i^{obs} - Y_i^{sim})^2}}{\sqrt{\sum_{i=1}^{n}(Y_i^{obs} - Y^{mean})^2}} \tag{12}$$

where, Y_i represents the observed value, Y_i' denotes the predicted value, i denotes the data sequence in the database, N represents the data counts, Y_i^{obs} signifies the observation data, Y_i^{sim} indicates the simulation data, and Y^{mean} signifies the mean value of the observed data.

Table 2. Performance Categories based on RSR and NSE Values by Moriasi et al [22]

Performance rating	RSR	NSE
Very good	0.00 ≤ RSR ≤ 0.50	0.75 < NSE ≤ 1.00
Good	0.50 < RSR ≤ 0.60	0.65 < NSE ≤ 0.75
Satisfactory	0.60 < RSR ≤ 0.70	0.50 < NSE ≤ 0.65
Unsatisfactory	RSR > 0.70	NSE ≤ 0.50

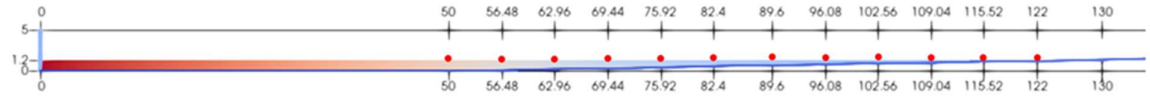

Fig. 7. 2D Cross-Sectional View of Setup 1 DualSPHysics Model

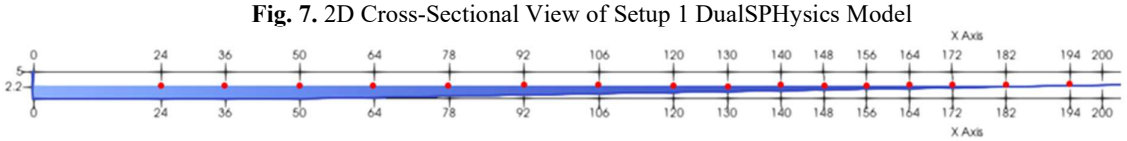

Fig. 8. 2D Cross-Sectional View of Setup 2 DualSPHysics Model

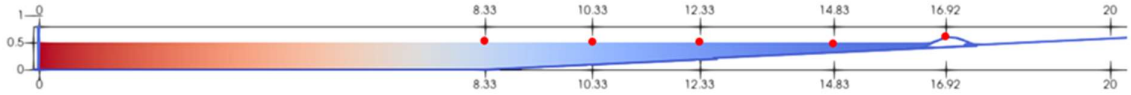

Fig. 9. 2D Cross-Sectional View of Setup 1 DualSPHysics Model

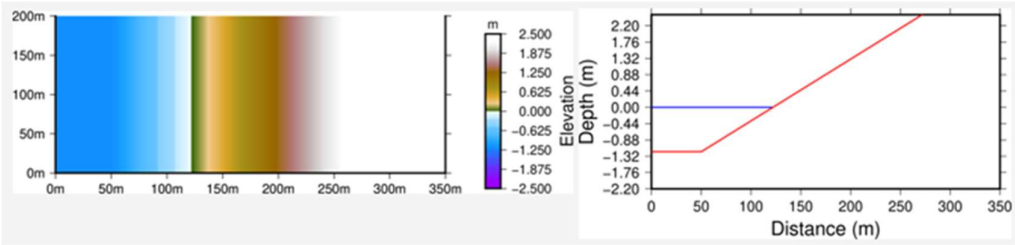

Fig. 10. a. Bathymetry *Setup* 1, b. *Slope Setup* 1

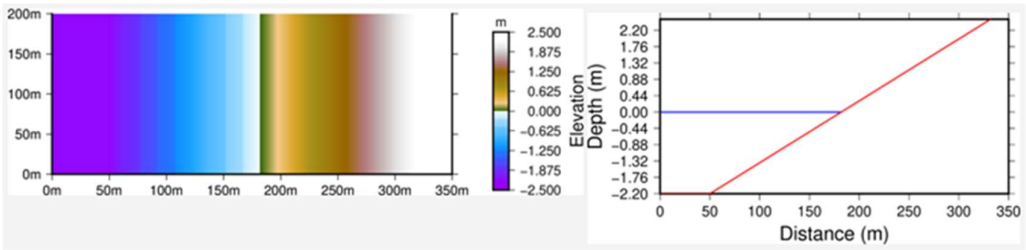

Fig. 11. a. Bathymetry *Setup* 2, b. *Slope Setup* 2

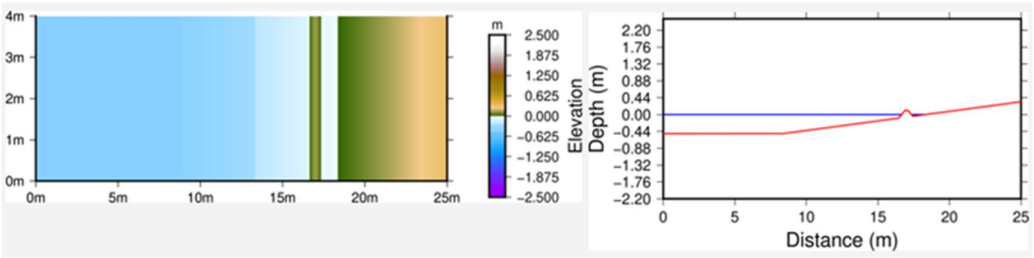

Fig. 12. a. Bathymetry *Setup* 3, b. *Slope Setup* 3

3 Result and Discussion

Simulation in the DualSPHysics program is highly sensitive to the value of the particle distance (dp), which in its application, represents the distributed fluid throughout the simulation domain. In the simulation conducted for setup 1, a dp value of 0.006 m was used, setup 2 employed a dp value of 0.008 m, and setup 3 utilized a dp value of 0.005 m. Meanwhile, in COMCOT a grid size system was employed, with grid size detail for setup 1, setup 2, and setup 3 being 0.1 m, 0.4 m, and 0.05 m, respectively.

3.1 Simulation Results of Solitary Wave Without a Seawall with a Water Depth of 1.2 m (Setup 1)

The results of the DualSPHysics simulation in Setup 1 using the KdV wave theory, align with the sensitivity test results, which indicate that the KdV wave theory perform better in simulating the experimental results in setups 2 and 3. However, the result for setup 1 are less satisfactory due to the disparity between the water depth and the flume length which are 1.2 m :300 m, repectively. This disparcity leads to a significant and inconsistent time lag when water enters the shallow area, with the simulation results being slower than the experiments. The timelag value used for η/h=0.338 is 10 in (t*). The inconsistency time lag (t*) in the DualSPHysics simulation results under shallower conditions is the main cause of leads to a significant increase in the occurring errors. Consequently, the DualSPHysics simulation results unsuitable for use, as indicated by their NSE and RSR values.

The results of the COMCOT simulation indicate better performance, with a minimum seven initial Wave Gauge (WG) achieving satisfactory results, whereas DualSPHysics only achieved satisfactory results for three initial WGs. In the COMCOT simulation results, at the observation point WG 82.4 m, the simulation showed unsatisfactory results based on the model comparison tests NSE and RSR. This phenomenon could be attributed to sedimentation in the water, which leads to wave reflection and diffraction, causing wave deformation.

Both of these phenomena can alter the speed of tsunami waves, thus affecting their timing and height. Consequently, as the water surface profile approaches the coastline, the influence of reflection and diffraction becomes more pronounced, as demonstrated from observation point WG 82.4 m to WG 122 m. As a result, the COMCOT simulation results cannot accurately represent the digitized flow profile.

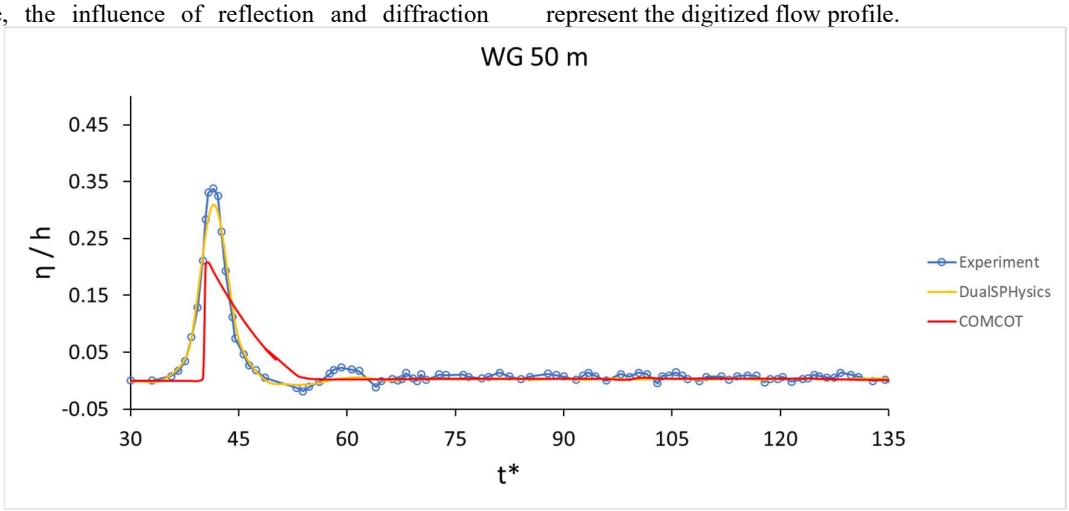

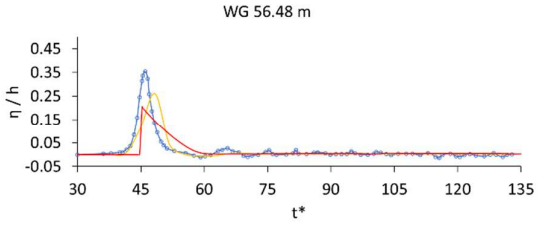

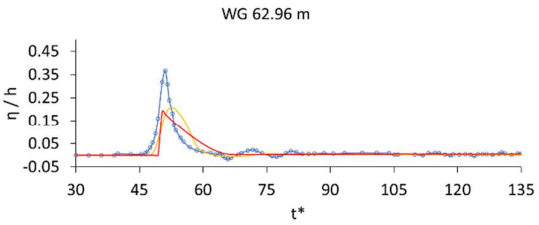

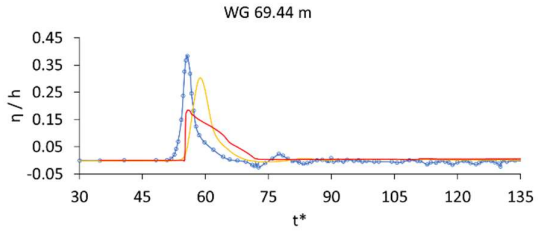

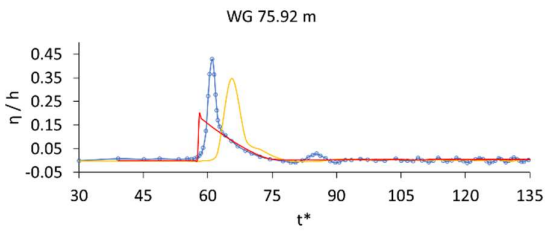

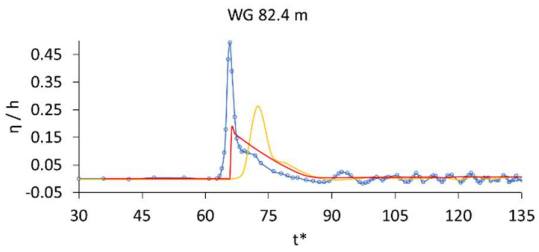

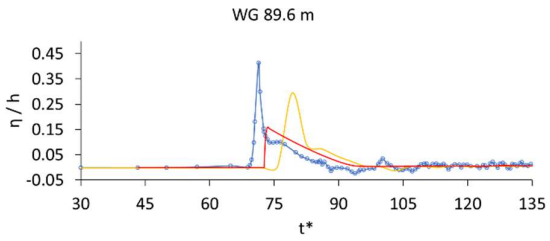

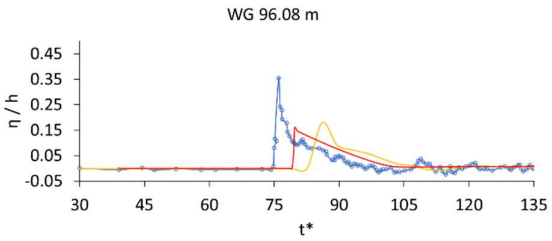

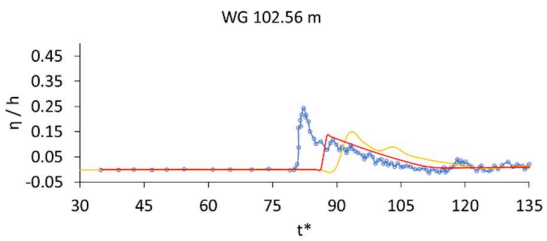

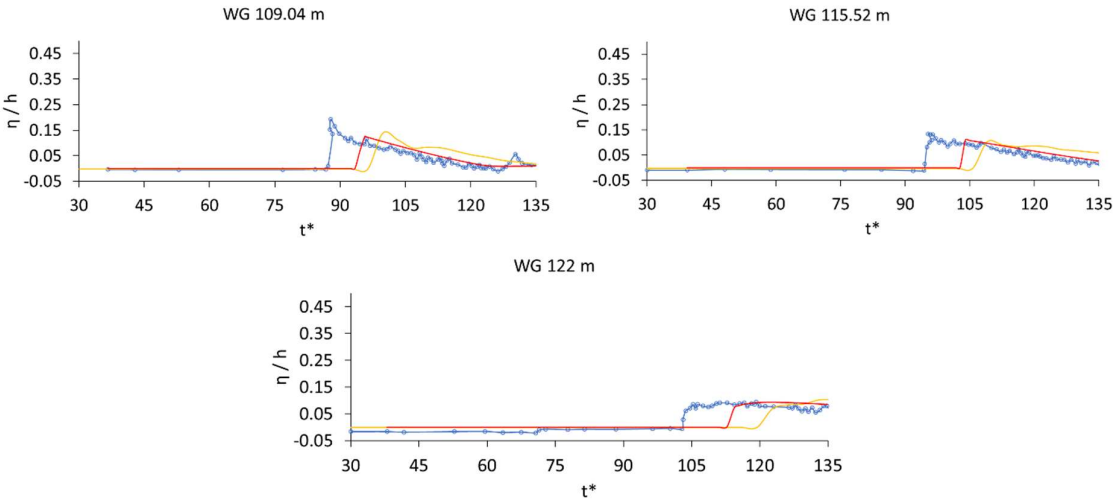

Fig. 13. Present Comparison Results of the DualSPHysics, COMCOT model, and Experimental Results for the Height and Water Surface Profile (WG 1 (50 m)-WG 12 (122 m)) in Setup 1 (η/h = 0.338)

Table 3. The Validation Results Error Value in Setup 1 (η/h = 0.338)

Validation Results		DualSPHysics		COMCOT	
Observation Point	Error	Solitary wave generation theory KdV	Performance Category (RSR and NSE)	Solitary wave generation theory Rayleigh	Performance Category (RSR and NSE)
WG 1 (50 m)	RMSE	0.014767	-	0.04322	-
	MAE	0.009122		0.02109	
	NSE	**0.961384**	Very good	0.67550	Good
	RSR	**0.196510**	Very good	0.56654	Good
WG 2 (56.48 m)	RMSE	0.051219	-	0.04984	-
	MAE	0.023626		0.02408	
	NSE	0.622218	Satisfactory	**0.64226**	Satisfactory
	RSR	0.614640	Satisfactory	**0.59450**	Good
WG 3 (62.96 m)	RMSE	0.043460	-	0.04200	-
	MAE	0.020586		0.02087	
	NSE	0.661681	Satisfactory	**0.68409**	Good
	RSR	0.581652	Satisfactory	**0.55830**	Good
WG 4 (69.44 m)	RMSE	0.079869	-	0.05358	-
	MAE	0.035434		0.02736	
	NSE	0.163335	Unsatisfactory	**0.62352**	Satisfactory
	RSR	0.914694	Unsatisfactory	**0.60987**	Satisfactory
WG 5 (75.92 m)	RMSE	0.094446	-	0.06030	-
	MAE	0.040977		0.02573	
	NSE	-0.147984	Unsatisfactory	**0.53202**	Satisfactory
	RSR	1.071440	Unsatisfactory	**0.67996**	Satisfactory
WG 6 (82.4 m)	RMSE	0.090624	-	0.07876	-
	MAE	0.036235		0.02857	
	NSE	-0.130817	Unsatisfactory	0.20123	Unsatisfactory
	RSR	1.063399	Unsatisfactory	0.88859	Unsatisfactory
WG 7 (89.6 m)	RMSE	0.071692	-	0.06202	-
	MAE	0.036445		0.02661	
	NSE	-0.378646	Unsatisfactory	-0.03164	Unsatisfactory
	RSR	1.174158	Unsatisfactory	1.01061	Unsatisfactory
WG 8 (96.08 m)	RMSE	0.077596	-	0.06319	-
	MAE	0.052313		0.03466	
	NSE	-0.494686	Unsatisfactory	-0.11007	Unsatisfactory
	RSR	1.222574	Unsatisfactory	1.04888	Unsatisfactory
WG 9 (102.52 m)	RMSE	0.073594	-	0.06576	-
	MAE	0.047383		0.03516	
	NSE	-0.553634	Unsatisfactory	-0.24111	Unsatisfactory
	RSR	1.246449	Unsatisfactory	1.10841	Unsatisfactory
WG 10 (109.04 m)	RMSE	0.065422	-	0.05250	-
	MAE	0.050818		0.03108	
	NSE	-0.966734	Unsatisfactory	-0.26676	Unsatisfactory
	RSR	1.402403	Unsatisfactory	1.11766	Unsatisfactory
WG 11 (115.52 m)	RMSE	0.065276	-	0.05333	-
	MAE	0.054589		0.03600	
	NSE	-1.751961	Unsatisfactory	-0.83655	Unsatisfactory
	RSR	1.658904	Unsatisfactory	1.34489	Unsatisfactory
WG 12 (122 m)	RMSE	0.053789	-	0.03960	-
	MAE	0.042846		0.02787	
	NSE	-0.744318	Unsatisfactory	0.05465	Unsatisfactory
	RSR	1.320726	Unsatisfactory	0.96307	Unsatisfactory

3.2 Solitary Wave Simulation Results Without a Seawall with a Water Depth of 2.2 m (Setup 2)

The simulation results obtained from DualSPHysics analysis in setup 2 differ from setup 1, where there was a significant time lag resulting in errors. The results of setup 2 are favorable because out of a total of 16 WG, only 2 did not meet the simulation standards and were considered unsatisfactory based on NSE and RSR values, which were at WG 182 m and 194 m. This is because at WG 182 m, there was a time lag of 4.628767 in (t*), and at WG 194 m, there was no change in water surface, indicating that with a dp value of 0.008 m, the wave runup had not reached WG 194 m, resulting in a η/h = 0 for both wave height and water surface profile. In setup 2, a time lag of 21.0755 in (t*) was observed at WG 24 m. The validation results, as shown in Table 4, indicate the values for RMSE, MAE, NSE, and RSR validation.

Based on the above figure, it can be observed that at the observation points from WG 148 m to WG 194 m, the performance of the COMCOT program is unsatisfactory, as indicated by the NSE and RSR model comparison tests. In the simulation results at x = 106 m, this is the point where the digitized water surface profile and the simulated water surface profile do not have the same height until WG 164 m. Therefore, it can be stated that the COMCOT program fails to replicate the height of tsunami waves. This can occur due to the same sedimentation process as in setup 1, which leads to the phenomena of wave reflection and diffraction, causing changes in flow velocity, influencing propagation time, and wave height. However, in this case, COMCOT is superior as it can simulate the run-up occurring at WG 194 m, despite a significant time lag.

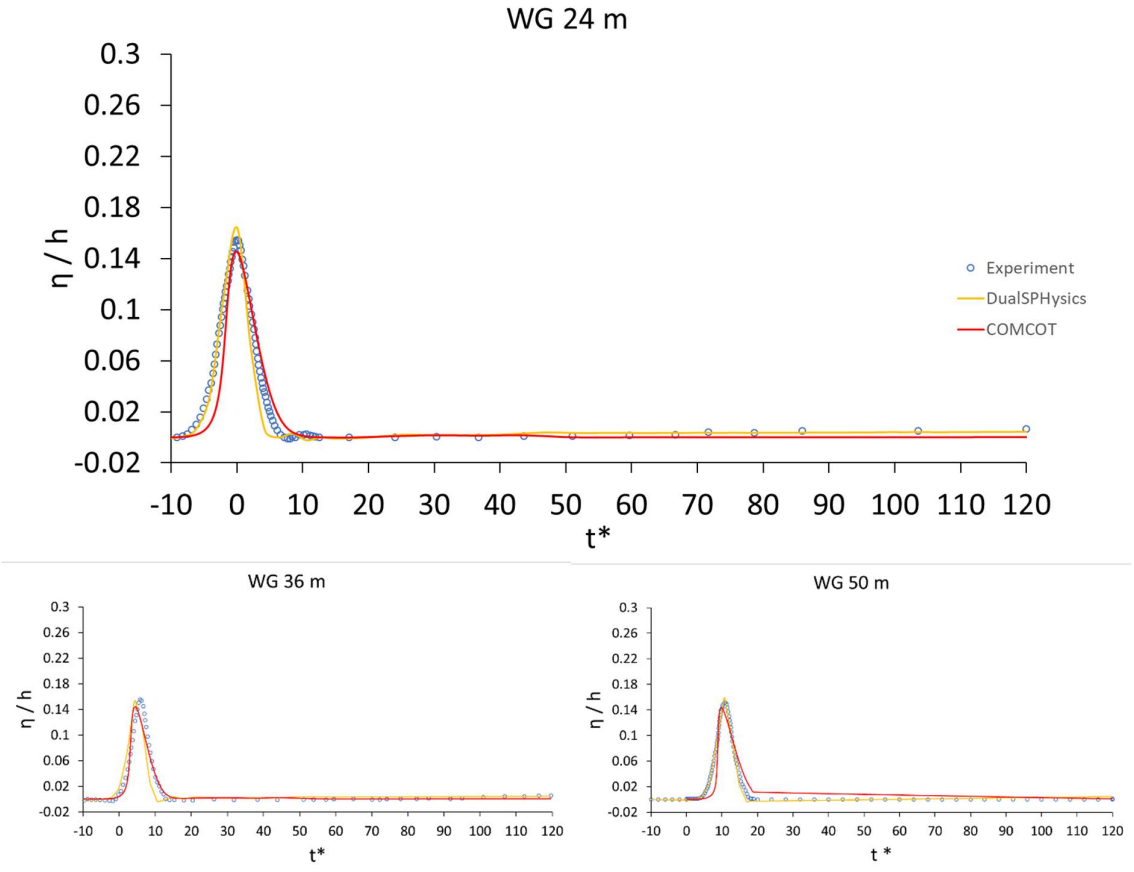

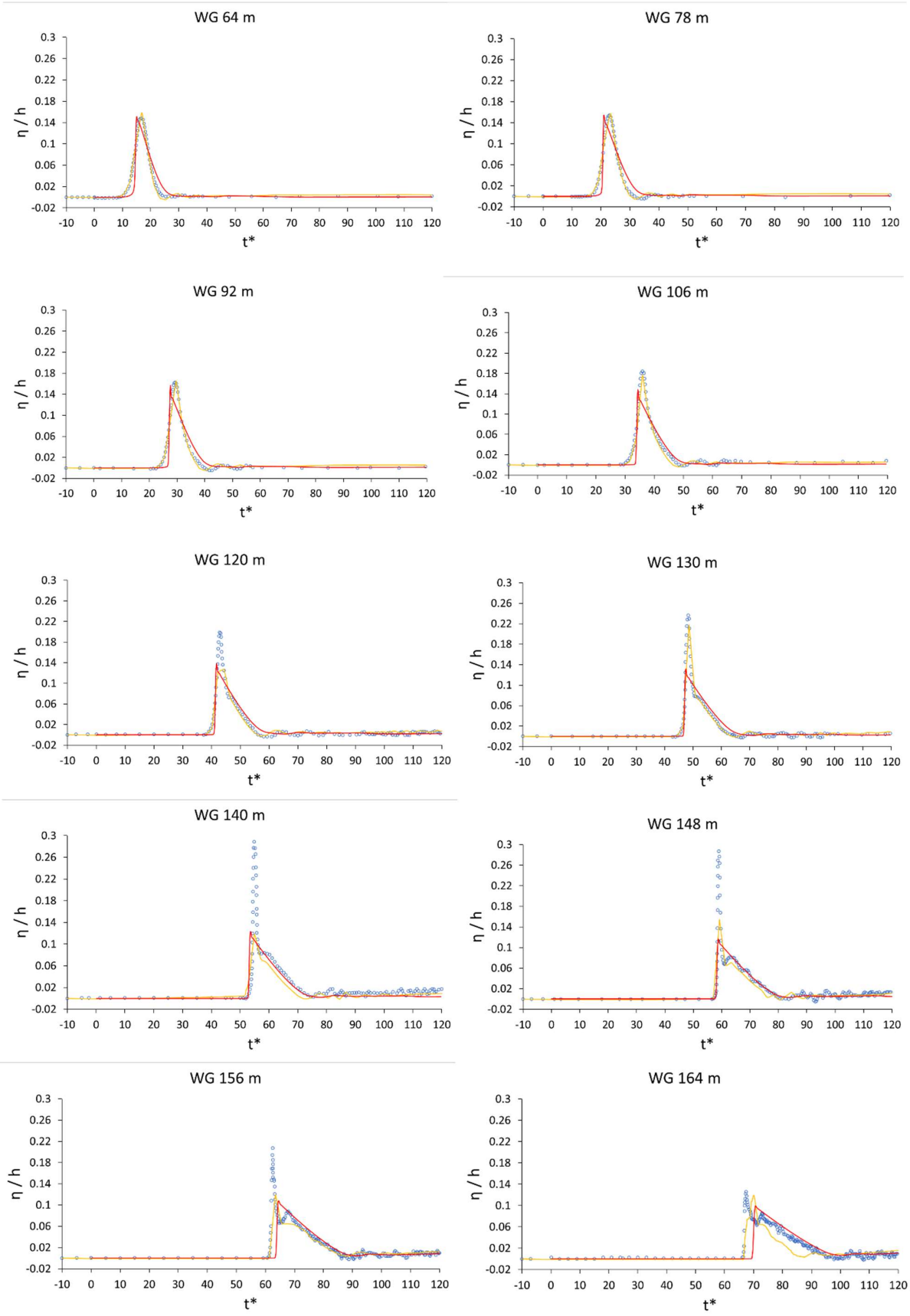
WG 64 m
WG 78 m
WG 92 m
WG 106 m
WG 120 m
WG 130 m
WG 140 m
WG 148 m
WG 156 m
WG 164 m
η / h
t*

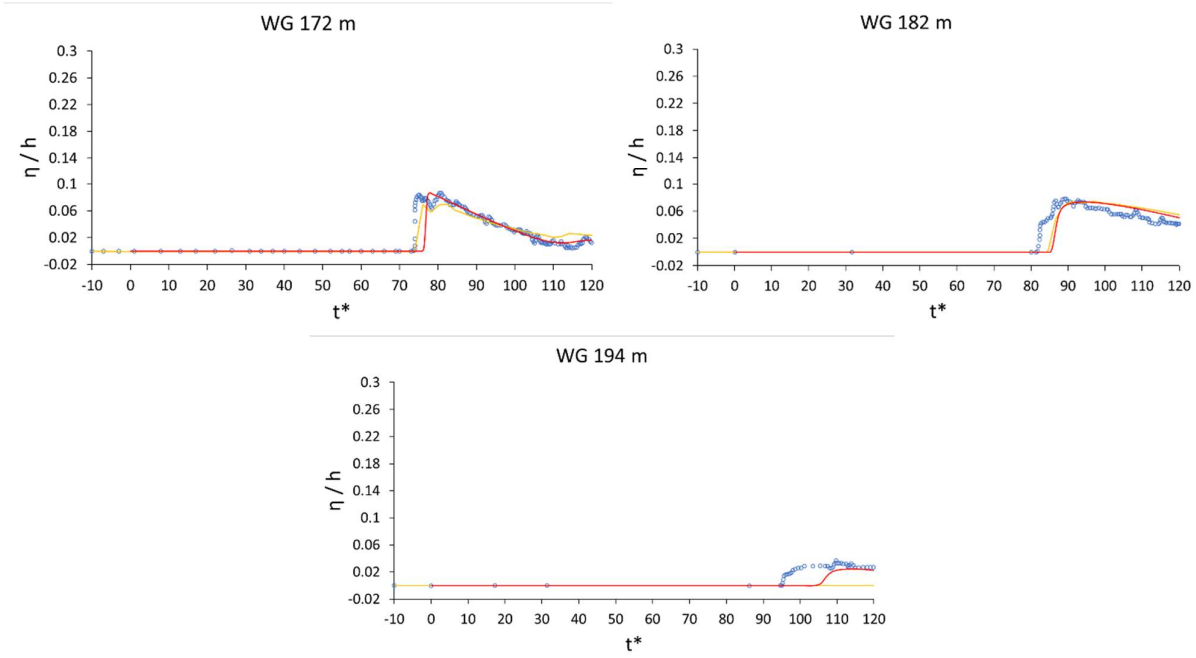

Fig. 14. Present Comparison Results of the DualSPHysics, COMCOT model, and Experimental Results for the Height and Water Surface Profile (WG 1 (24 m)-WG 16 (194 m)) in Setup 2 (η/h = 0.152)

Table 4. The Validation Results Error Value in Setup 2 (η/h = 0.152)

Validation Results		**DualSPHysics**		**COMCOT**	
Observation Point	Error	Solitary wave generation theory	Performance Category (RSR and NSE)	Solitary wave generation theory	Performance Category (RSR and NSE)
		KdV		Rayleigh	
WG 1 (24 m)	RMSE	0.01233	-	0.01714	-
	MAE	0.00800		0.01186	
	NSE	**0.94806**	Very good	0.89960	Very Good
	RSR	**0.22791**	Very good	0.31508	Very Good
WG 2 (36 m)	RMSE	0.02279	-	0.01374	-
	MAE	0.01573		0.00848	
	NSE	0.80219	Very good	**0.92805**	Very Good
	RSR	0.44476	Very good	**0.26619**	Very Good
WG 3 (50 m)	RMSE	0.00649	-	0.02087	-
	MAE	0.00502		0.01621	
	NSE	**0.98453**	Very good	0.84023	Very Good
	RSR	**0.12438**	Very good	0.39688	Very Good
WG 4 (64 m)	RMSE	0.00489	-	0.01954	-
	MAE	0.00376		0.01310	
	NSE	**0.99107**	Very good	0.85743	Very Good
	RSR	**0.09450**	Very good	0.37488	Very Good
WG 5 (78 m)	RMSE	0.00557	-	0.01888	-
	MAE	0.00411		0.01258	
	NSE	**0.98924**	Very good	0.87662	Very Good
	RSR	**0.10371**	Very good	0.34850	Very Good
WG 6 (92 m)	RMSE	0.00741	-	0.02032	-
	MAE	0.00519		0.01352	
	NSE	**0.98286**	Very good	0.87103	Very Good
	RSR	**0.13091**	Very good	0.35622	Very Good
WG 7 (106 m)	RMSE	0.01054	-	0.02406	-
	MAE	0.00716		0.01515	
	NSE	**0.96692**	Very good	0.82758	Very Good
	RSR	**0.18188**	Very good	0.41217	Very Good
WG 8 (120 m)	RMSE	0.02237	-	0.02106	-
	MAE	0.01430		0.01114	
	NSE	**0.90250**	Very good	0.85766	Very Good
	RSR	**0.31225**	Very good	0.37559	Very Good

WG 9 (130 m)	RMSE	0.01773	-	0.02849	-
	MAE	0.00926		0.01383	
	NSE	**0.92224**	Very good	0.79922	Very Good
	RSR	**0.27885**	Very good	0.44602	Very Good
WG 10 (140 m)	RMSE	0.04520	-	0.04645	-
	MAE	0.02328		0.02364	
	NSE	**0.61649**	Satisfactory	0.59692	Satisfactory
	RSR	**0.61928**	Satisfactory	0.63389	Satisfactory
WG 11 (148 m)	RMSE	0.03191	-	0.06132	-
	MAE	0.01486		0.02409	
	NSE	**0.74029**	Good	0.08128	Unsatisfactory
	RSR	**0.50962**	Good	0.97648	Unsatisfactory
WG 12 (156 m)	RMSE	0.02670	-	0.04897	-
	MAE	0.01130		0.02056	
	NSE	**0.66007**	Good	-0.03669	Unsatisfactory
	RSR	**0.58304**	Good	1.06627	Unsatisfactory
WG 13 (164 m)	RMSE	0.02060	-	0.03129	-
	MAE	0.01403		0.01564	
	NSE	0.56728	Satisfactory	0.34775	Unsatisfactory
	RSR	0.65782	Satisfactory	0.95649	Unsatisfactory
WG 14 (172 m)	RMSE	0.01681	-	0.02593	-
	MAE	0.01078		0.01211	
	NSE	**0.61027**	Satisfactory	0.13856	Unsatisfactory
	RSR	**0.62429**	Satisfactory	0.95950	Unsatisfactory
WG 15 (182 m)	RMSE	0.01778	-	0.01984	-
	MAE	0.01423		0.01437	
	NSE	0.01497	Unsatisfactory	-0.22674	Unsatisfactory
	RSR	0.99249	Unsatisfactory	1.10192	Unsatisfactory
WG 16 (194 m)	RMSE	0.02492	-	0.01362	-
	MAE	0.02243		0.01059	
	NSE	-4.21820	Unsatisfactory	-0.55825	Unsatisfactory
	RSR	2.28434	Unsatisfactory	1.23435	Unsatisfactory

3.3 Solitary Wave Simulation Results Using Seawall (Setup 3)

The results obtained from DualSPHysics in simulating Setup 3 are satisfactory, as evidenced by the water height and water surface profile closely matching the experimental data. Furthermore, the validation results based on NSE and RSR values show the minimum values at WG 8.33 m, indicating that the measurements at all WGs yielded good results.

The simulation results obtained from COMCOT for Setup 3 did not demonstrate satisfactory performance in the model validation using NSE and RSR. This could be attributed to the inability of the COMCOT program to simulate the overtopping process on the seawall, resulting in the program's failure to produce consistent results as the waves began to impact the seawall. Consequently, the water surface profile shown did not match between the digitized data and the simulation results. A detailed water surface profile can be observed in Figure 14 below. At the observation point of WG 8.33 m, the simulation results were able to match the time and wave height parameters up to the second wave. However, when the waves began to hit the seawall, the water surface profile no longer exhibited accurate results. Starting at WG 10.33 m, a difference in wave velocity occurred between the digitized data and the simulation results, indicating that the overtopping process generated by the COMCOT program was not accurate. This discrepancy may be attributed to the program's inability to adapt to the mechanisms of changing water surface profiles and flow velocities impacting the seawall.

In the given simulation setup, DualSPHysics outperforms COMCOT when it comes to coastal structures as it can accurately depict the results of tsunami wave impact on seawalls. Furthermore, as seen in Figure 14, DualSPHysics provides better results for wave reflections compared to COMCOT, which tends to produce extreme retreats in water surface elevation as observed in the experiments. The second overtopping event, however, was not simulated by either DualSPHysics or COMCOT. This limitation may arise from the use of a particle distance (dp) value of 0.005 m in DualSPHysics and a grid size of 0.05 m in COMCOT, which may need to be reduced to simulate the actual experimental conditions more accurately. Therefore, to achieve improved results, further testing with smaller dp values in DualSPHysics and smaller grid sizes in COMCOT may be necessary.

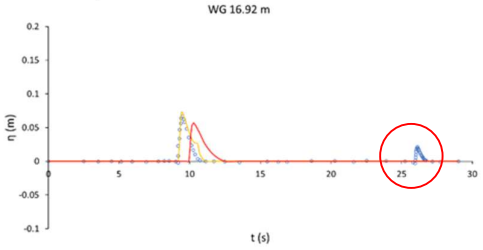

Fig. 15. Second Overtopping Event Not Simulated in DualSPHysics and COMCOT Results.

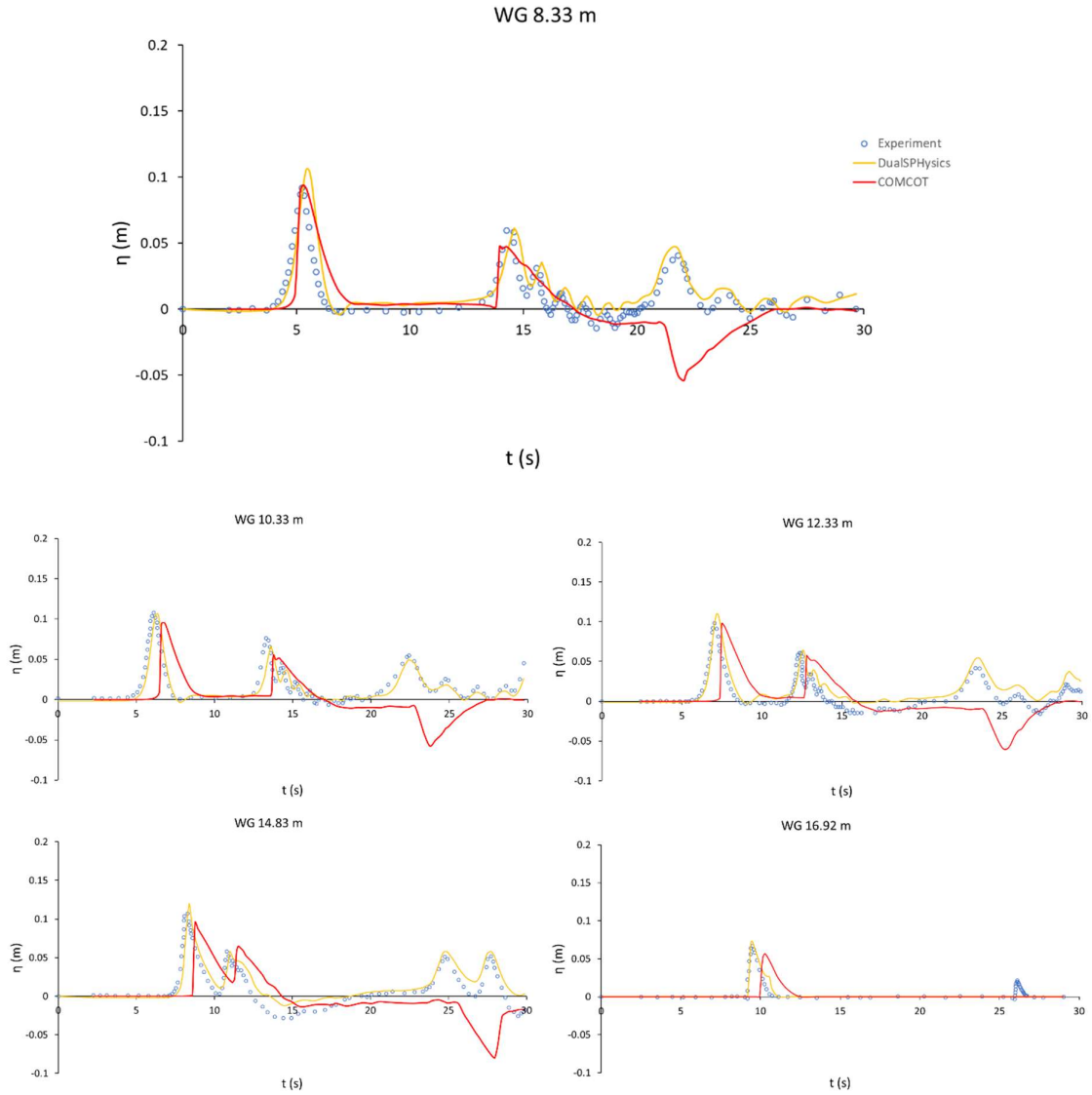

Fig. 16. Present Comparison Results of the DualSPHysics, COMCOT model, and Experimental Results for the Height and Water Surface Profile (WG 1 (8.33 m)-WG 5 (16.92 m)) in Setup 3

Table 5. The Validation Results Error Value in Setup 3

Validation Results		DualSPHysics		COMCOT	
Observation Point	Error	Solitary wave generation theory	Performance Category (RSR and NSE)	Solitary wave generation theory	Performance Category (RSR and NSE)
		KdV		Rayleigh	
WG 1 (8.33 m)	RMSE	0.01340	-	0.02357	-
	MAE	0.00970		0.01506	-
	NSE	**0.63679**	Satisfactory	-0.12157	Unsatisfactory
	RSR	**0.60267**	Satisfactory	1.05563	Unsatisfactory
WG 2 (10.33 m)	RMSE	0.01364	-	0.04184	-
	MAE	0.00965		0.03078	-
	NSE	**0.77558**	Very good	-1.10982	Unsatisfactory
	RSR	**0.47373**	Very good	1.44602	Unsatisfactory
WG 3 (12.33 m)	RMSE	0.01646	-	0.03483	-
	MAE	0.01563		0.02641	-
	NSE	**0.66323**	Good	-0.90242	Unsatisfactory
	RSR	**0.58032**	Good	1.38566	Unsatisfactory
WG 4 (14.38 m)	RMSE	0.01664	-	0.04785	-
	MAE	0.01317		0.03470	-
	NSE	**0.73603**	Good	-1.18359	Unsatisfactory
	RSR	**0.51378**	Good	1.47044	Unsatisfactory
WG 5 (16.92 m)	RMSE	0.00885	-	0.02165	-
	MAE	0.00592		0.01535	-
	NSE	**0.76702**	Very good	-0.39431	Unsatisfactory
	RSR	**0.48268**	Very good	1.17169	Unsatisfactory

3.4 Stepped-face wall (SW) Seawall in the DualSPhysics model.

The results of the DualSPHysics simulation have yielded favorable outcomes in simulating the seawall, enabling further research in this area. This study focuses on the volume of overtopping water and the overtopping height. The choice of Solitary Wave (SW) is based on the research conducted by Dang et al. [23], which demonstrated that this type of SW can reduce the overtopping effects compared to a trapezoidal wall (TW) seawall, as in setup 3. Additionally, SW seawalls are easier to maintain in case of damage caused by overtopping effects [23]. The wave generation theory employed in this study is the KdV theory.

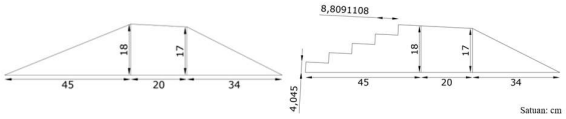

(a) (b)

Fig. 17. Seawall Dimensions: (a) Trapezoidal Wall (TW), (b) Stepped-Face Wall (SW).

Based on Figure 17, the results of measurements for both types of seawalls indicate that the maximum overtopping height occurred at t = 9.4 seconds, with a height of 0.078006 m for the TW type and 0.077317 m for the SW type. The difference in overtopping between the two types is small, at only 0.883%. This means that the modification of the seawall's front shape has a negligible impact on overtopping, considering the wave height and wave depth ratio (H0/h) of 0.2. This can be attributed to the relatively high wave height generated, which reduces the significant influence of the seawall in reducing overtopping height.

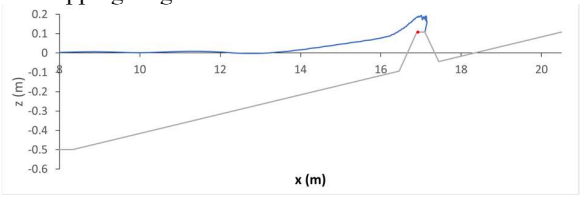

(a)

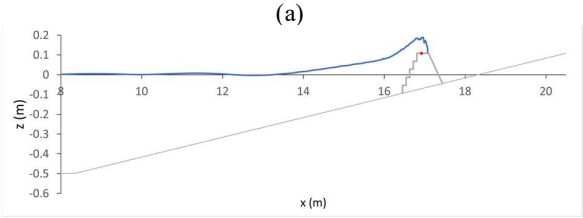

(b)

Fig. 18. Overtopping at t = 9.4 seconds: (a) Trapezoidal Wall (TW), (b) Stepped-Face Wall (SW).

In the process of measuring the overtopping volume, additional observation points or WG points are needed, including WG 6 located at x = 17.6938 m, represented by the red triangle in Figure 18. Furthermore, an extended duration of time (t) in seconds is required, with an additional time span of 45 seconds to ensure that the water in the tank becomes calm without significant changes in the surface elevation.

With the water level results in the tank, the trapezoidal wall (TW) seawall has a height of 0.07001 m, while the seawall type SW has a height of 0.06323 m. This indicates that the SW type seawall can reduce the volume of overtopping water by 9.682%. The measurement results can be seen in Figure 18. When comparing the nearly equal overtopping heights between TW and SW types, the influencing factor that makes SW seawall more effective is the speed and duration of overtopping. From Figure 19, it can be observed that overtopping occurs more quickly with the SW seawall compared to the TW type. Based on the graphical output results, it can be concluded that the overtopping height is lower for the SW seawall. This reduction in height leads to a 9.682% decrease in volume.

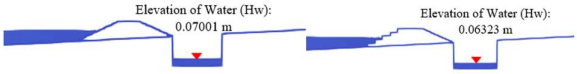

(a) (b)

Fig. 19. Height Measurement Results for Volume: (a) Trapezoidal Wall (TW): 0.07001 m, (b) Stepped-Face Wall (SW): 0.06323 m.

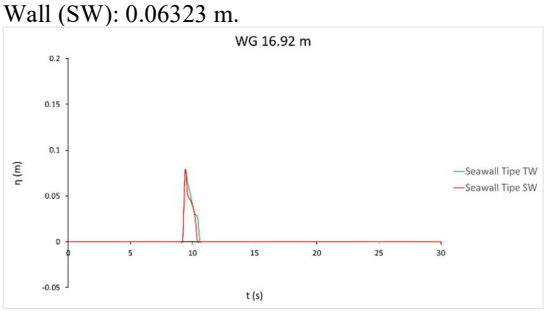

Fig. 20. Comparison of simulations based on DualSPHysics Model Sensitivity Test and Experimental Height and Water Surface Profile (WG 5 (16.92 m)) in Setup 3 for Trapezoidal Wall and Stepped-Face Wall Seawall.

4 Conclusion

In this study it can be concluded that both DualSPhysics and the COMCOT program have the capability to simulate the propagating of tsunami waves towards land. When conducting simulations with the DualSPhysics program, the presence of a parameter known as “dp” significantly influences the accuracy of the simulation. Therefore, in setup 1, setup 2 and setup 3 respectively 0.006 m, 0.008 m and 0.005 m are used. So that the simulation results using DualSPhysics show quite good speed and altitude values based on the test results of the NSE and RSR models. In setup 1 there are the three wave gauges positions at 50 m, 56.48 m, and 62.96 m obtained NSE values of 0.961, 0.622, and 0.661 respectively which values are > 0.50. While the RSR model test was 0.196, 0.614 and 0.581 which value is < 0.70. On the other hand, the COMCOT program involves the consideration of grid size parameters (Δx & Δy) and time step (Δt), which exect an influance on the simulation’s accuracy. In setup 1, setup 2, and setup 3 respectively 0.1 m, 0.4 m, and 0.05 m, while the time step

is 0.01 s, 0.01 s, and 0.001 s. As the result, the simulation outcomes using COMCOT exhibit favorable speed and altitude values, as indicated by the NSE and RSR model test results. In setup 1, the initial three wave gauges positioned at 50 m, 56.48 m, and 62.96 m obtained NSE values of 0.675, 0.642 and 0.684 respectively, which values are > 0.50. While the RSR model test was 0.566, 0.594 and 0.558 respectively, where these values were <0.70. However, it is worth nothing that the simulating of tsunami overtopping on the seawall using COMCOT program fails to produce satisfactory results. This issue may arise due to the program's may inability to equate the profile of the water surface when waves first impact the seawall. In contrast, the simulation of tsunami wave overtopping on the seawall using the DualSPHysics program yields highly favourable results.

References

[1] Synolakis, C., & Bernard, E. (2006). Tsunami science before and beyond Boxing Day 2004. *Philos. Trans. R. Soc. A*, 364, 2231–2265.

[2] Pelinovsky, E. N. and Poplavsky, A.: Simplified model of tsunami generation by submarine landslides, Phys. Chem. Earth, 21, 13– 17, 1996.

[3] Mori, N., & Takahashi, T. (2012). The 2011 Tohoku Earthquake Tsunami Joint Survey Group (2012) Nationwide post event survey and analysis of the 2011 Tohoku earthquake tsunami. *Coast. Eng.*, 54, 1–27.

[4] Yalciner, A., Ozer, C., Zaytsev, A., Suppasri, A., Mas, E., Kalligeris, N., Synolakis, C. (2011). Field survey on the coastal impacts of March 11, 2011 Great East Japan Tsunami. In Proceedings of the Seismic Protection of Cultural Heritage. *In Proceedings of the Seismic Protection of Cultural Heritage.* Turkey: Antalya.

[5] Suppasri, A., Shuto, N., Imamura, F., Koshimura, S., Mas, E., & Yalciner, A. C. (2012). Lessons Learned from the 2011 Great East Japan Tsunami: Performance of Tsunami Countermeasures, Coastal Buildings, and Tsunami Evacuation in Japan. *Pure and Applied Geophysics*, 994-1018.

[6] Young, Y., Xiao, H., & Maddux, T. (2010). Hydro-and morpho-dynamic modeling of breaking solitary waves over a fine sand beach. *Part I: Experimental study. Mar. Geol. 2010*, 107–118.

[7] Rasyif, T. M., Saputra, F., Widia, & Akmal. (2020). Simulasi Aliran Dam-Break Menggunakan Program DualSPHysics. *Jurnal Telknik Sipil*, Vol.9 No.2.

[8] Atmika, I. K. (2016). *Metode Numerik.* Denpasar: Universitas Udayana.

[9] Li, Y., Ma, Y., Deng, R., Jiang, D., & Hub, Z. (2019). Research on dam-break induced tsunami bore acting on the triangular breakwater based on high order 3D CLSVOF-THINC/WLIC-IBM approaching. *Ocean Engineering 182* , 645–659.

[10] Benazir, R. Triatmadja, A. P., Yuwono, N., & dkk. (2019). The Behavior Of A Tsunami-Like Wave Produced By Dam Break And Its Run-Up On 1: 20 Slope. *Sci. Tsunami Hazards, vol. 38, no. 2*.

[11] H. Chanson, S. A. (2000). Experimental Investigations of Wave Runup Downstream of Nappe Impact: Applications toFlood Wave Resulting from Dam Overtopping and Tsunami Wave Runup. *Coastal/Ocean Eng. Rep. No. COE00-2. Dept. Archit. Civ. Eng., Toyohashi Univ. Technol. Japan*.

[12] H. P. Lin, P. L. (2014). Solitary wave theory and its applications to coastal disaster mitigation. *Journal of Marine Science and Technology, vol. 22, no. 2*, 147-157.

[13] Altomare, C., Y. Oshima, X. C., Crespo, A. J., & Suzuki, T. (2015). Study of the overtopping flow impacts on multifunctional sea dikes in shallow foreshores with an hybrid numerical model. *in 36th IAHR World Congress*, 1-11.

[14] Trimulyono, A. (2018). Validasi Gerakan Benda Terapung Menggunakan Metode Smoothed Particle Hydrodynamics. *KAPAL, Vol. 15, No. 2 Juni*, 38-43.

[15] Wang, X. (2009). User manual for COMCOT version 1.7 (First Draft).

[16] Ratuluhain, E. S., & Noya, Y. A. (2022). Rekonstruksi Tsunami Mentawai dengan Menggunakan COMCOT v1.7. *NEKTON: Jurnal Perikanan dan Ilmu Kelautan*, 54-62.

[17] Al'ala. M. (2015). NUMERICAL SIMULATION OF UJONG SEUDEUN LAND SEPARATION CAUSED BY THE 2004 INDIAN OCEAN TSUNAMI, ACEH-INDONESIA. *Tsunami Society International*, 159-172.

[18] T. M. Rasyif, "DATA BASE DEVELOPMENT OF ESTIMATED TIME OF," 2014.

[19] Huang, J. X., Qu, K., Li, X. H., & Lan, G. Y. (2022). Performance Evaluation of Seawalls in Mitigating a Real-World TsunamiWave Using a Nonhydrostatic NumericalWave Model. *J. Mar. Sci. Eng. 2022, 10, 796*, 1-21.

[20] Hsiao, S.-C., Lin, T.-W. H.-C., & Yu-Hsuan. (2008). On the evolution and run-up of breaking solitary waves on a mild sloping beach. *Coastal Engineering 55*, 975–988.

[21] Hunt, A., Hall, S. E., & Term, M. (2003). *Extreme Waves, Overtopping and Flooding at Sea Defences.A thesis submitted in partial fulfilment for the degree of Doctor of Philosophy at the University of Oxford.* Oxford: Department of Engineering Science University of Oxford Parks Road Oxford OX1 3PJ.

[22] Moriasi, D., Liew, M. W., Arnold, J., & Bingner, R. (2007). Model Evaluation Guidelines for Systematic Quantification of Accuracy in Watershed Simulations. *Transactions of the ASABE (American Society of Agricultural and Biological Engineers)*, 885-900.

[23] Dang, B.-L., Nguyen-Xuan, H., & Wahab, M. A. (2021). Numerical Study on Wave Forces and Overtopping over various seawall structures using advance SPH-based method. *Engineering Structures 226*, 226.